

THE 4TH INTERNATIONAL CONFERENCE ON ALUMINUM ALLOYS

NUCLEATION OF α -Al ON GRAIN-REFINING PARTICLES STUDIED IN CRYSTALLIZATION OF AMORPHOUS Al-ALLOYS

P. Schumacher and A.L. Greer

University of Cambridge, Department of Materials Science and Metallurgy, Pembroke Street, Cambridge CB2 3QZ (UK)

Abstract

The low atomic mobility in metallic glasses permits the microscopical study of nucleation on added particles. The nucleation of α -Al by conventional grain-refining additions such as Al_3Ti and TiB_2 has been studied in amorphous $\text{Al}_{85}\text{Y}_8\text{Ni}_5\text{Co}_2$ (at.%). In samples with excess Ti copious formation of α -Al has been observed on TiB_2 particles coated with a layer of Al_3Ti ; without excess Ti the Al_3Ti is not observed and the nucleation efficiency is greatly reduced.

Introduction

In conventional aluminium castings grain-refiner additions are used to promote a uniform microstructure throughout an ingot. The refiner additions are usually in the form of an aluminium rod containing TiB_2 particles and Al_3Ti particles in an aluminium matrix. The nucleation mechanism of boride and aluminide additions has been widely studied, but remains not fully understood. There is a peritectic reaction (liquid + Al_3Ti \rightarrow α -Al) at 3° C above the melting point of pure aluminium. This reaction is believed to be a powerful nucleation mechanism to promote the formation of α -Al on Al_3Ti particles [1]. However, grain refinement can be observed in very dilute aluminium alloys (0.03 – 0.08 wt%Ti) even beyond the expected dissolution times of larger Al_3Ti particles [2]. The chemically inert TiB_2 particles are not expected to dissolve as quickly as the aluminide particles and have been found empirically to enhance the grain-refining performance when an excess Ti level is present [3]. Various mechanisms have been suggested in which boride particles might act to preserve Al_3Ti locally. The proposed mechanisms are:

1. a surrounding shell of borides [4,5];
2. survival in cavities [6];
3. an adsorption layer on borides [7].

However, it is not possible to observe directly the actual nucleation mechanism in dilute aluminium alloys, since any microstructural investigation is hindered by the high atomic mobility and non-isothermal casting conditions. Observations of the as-cast microstructure are often inconclusive because the microstructure depends not only on nucleation, but also on subsequent growth.

Crystallization of an amorphous alloy (obtained by melt-spinning) can be regarded as a slow-motion analogue of crystallization from a melt. An estimation of the atomic mobilities for both reactions, which are inversely related to the viscosities, suggests reaction kinetics for devitrification 10^{16} times slower than for crystallization from a melt. The rate-limiting step in crystallization from a dilute melt is determined by heat flow, while in crystallization from a glass it is determined by solute transport or interfacial kinetics. Both cases represent an undercooled liquid, though the glass is highly undercooled and has a higher solute content. A suitable alloy for the study of nucleation on grain refining particles has to fulfil various conditions [8]. The alloy has to have sufficient glass-forming ability that after melt-spinning only negligible crystalline volumes can be found on added sites; it has to show α -Al during devitrification, and the nucleation density in the amorphous matrix has to be sufficiently low in order to distinguish between nucleation on added sites and nucleation in the matrix which is unaffected by added sites. The observation of nucleation events is favoured by a slow growth rate and a time delay between the nucleation onset on added sites and nucleation in the matrix. Previous work [9,10] has been shown that amorphous $\text{Al}_{85}\text{Y}_8\text{Ni}_5\text{Co}_2$ (at.%) (which is known to be relatively stable [11,12]) can be used to study the action of commercial grain-refiner additions. In this work it will be shown how excess Ti levels can affect the nucleation of α -Al on boride particles.

Experimental methods

Two alloys for melt-spinning were prepared *in situ* in the melt-spinning crucible (BN) from conventional aluminium grain-refiner rods (London & Scandinavian Metallurgical Co.) and a master alloy prepared by arc melting on a copper hearth under inert (argon) atmosphere from aluminium (99.999%), yttrium (99.99%), nickel (99.99%) and cobalt (99.99%). In the grain-refiner rod and in the final alloy, the boron is expected to be entirely in TiB_2 particles, leaving any excess Ti dissolved in the matrix. The solute content of the master alloy was selected so that the matrix composition of the alloys studied here matches as closely as possible the $\text{Al}_{85}\text{Y}_8\text{Ni}_5\text{Co}_2$ used in an earlier devitrification study [12] without added particles. Two ribbons were prepared

with added grain-refiner rod: I with rod of the well known composition Al-5wt.%Ti-1wt.%B; and II with Al-4.5wt.%Ti-1.8wt.%B, the Ti to B ratio in the latter rod being close to stoichiometric for TiB₂. Thus the final overall compositions (at.%) of the two ribbons were {Al₈₅[Y₈Ni₅Co₂]_{15-x} + (excess Ti)_x }_{100-y} + {TiB₂}_y with $x = 0.13$ and $y = 0.32$ for ribbon I and $x \sim 0$ and $y = 0.16$ for ribbon II. Approximately 10% of the aluminium content of the matrix comes from the grain-refiner rod in ribbon I (5%, ribbon II). The melt-spinning was carried out in inert atmosphere (helium) with a wheel speed of 44 m s⁻¹. The melt was held at 1020° C (measured with a single-colour pyrometer) for 10 s before ejection. Samples from both ribbons were heat treated in a differential scanning calorimeter (DSC) and the structure analysed by X-ray diffraction (XRD). Samples for transmission electron microscopy (TEM) were prepared by electropolishing using 4% perchloric acid in ethanol at -25° C. Energy-dispersive X-ray (EDX) analysis was used with Philips 400 microscope.

Results and Discussion

Microstructure of the as-quenched samples

In the as-quenched state of both ribbons particles can be observed which exhibit facets and have a hexagonal structure, electron diffraction indicating c/a -ratios of 1.01 to 1.06, close to the ratios of AlB₂ (1.083) and TiB₂ (1.066). In earlier work [10] boron was detected in these particles in thin areas of TEM samples using a microprobe. These particles most likely correspond to the (Ti_{1-x}Al_x)B₂ phase reported in grain-refining master alloys by Johnson and Bäckerud [13]. The estimated density of the particles is $8 \times 10^{15} \text{ m}^{-3}$ (from TEM). In ribbon I ($x = 0.13$, $y = 0.32$) a microstructure evolves from the particles which was not observed in the previous study of the alloy without grain-refining additions. On the boride particles, as shown in the TEM micrograph of Figure 1 a), for a particle with its $\langle 110 \rangle$ zone axis tilted parallel to the electron beam, small α -Al crystals (0.1 μm) have nucleated during the quench. This indicates that for this ribbon the quench-rate was not sufficient to avoid copious nucleation and some subsequent growth of aluminium. In Figure 1 the boride particle itself is not the actual nucleating substrate for aluminium. It is surrounded by a dark layer (arrows) which becomes more apparent in Figure 1 b) in dark-field-TEM with the objective aperture on the $\{111\}$ spot of aluminium. As pointed out in previous work [9], the thickness of this layer and the amount of α -Al on it are dependent on melt superheat and quenching rate. It is noteworthy that more than one Al-crystal is lit in the dark-field-TEM in Figure 1 b) suggesting an orientation relationship between aluminium and the boride on which aluminium can be observed on $\{001\}$ faces. In selected area diffraction of the boride particle in Figure 1, together with the layer and the aluminium crystals, parts of the characteristic diffraction patterns of the $\langle 110 \rangle$ TiB₂ (1), the $\langle 110 \rangle$ Al (3) and $\langle 110 \rangle$ Al₃Ti (2) become apparent as shown in Figure 2,

when the particle is slightly tilted off the $\langle 110 \rangle$ TiB_2 zone axis. Since the c/a ratio for Al_3Ti ($c/a = 2.23$) is approximately 2, the $\{112\}$ planes are pseudo close-packed and the directions $\langle 110 \rangle$ (and $\langle 201 \rangle$) within these planes are close-packed. Figure 2 shows that the orientation relationships between the phases are here:

$$\{001\} \langle 110 \rangle \text{TiB}_2 \parallel \{112\} \langle 110 \rangle \text{Al}_3\text{Ti} \parallel \{111\} \langle 110 \rangle \text{Al}.$$

Although the close-packed planes in each phase are thus parallel, misorientations of up to 2° have been found in earlier study [10]. The relationship found here between $\alpha\text{-Al}$ and TiB_2 is the same as that recently reported by Kim, Cantor, Griffith and Jolly [14] in melt-spun grain-refiner master alloys, though they did not observe any intermediate Al_3Ti layer. EDX-analysis reveals Al, Ti and Ta in the layer [9]. With aluminium, tantalum can form Al_3Ta , which is isomorphous with Al_3Ti and has similar lattice parameters leading to total solubility of Ta in Al_3Ti . The source of Ta is not known but is believed to come from the refiner rod. The absence of separate Al_3Ti particles is consistent with such particles originally present in the grain-refining rod dissolving in the melt during processing.

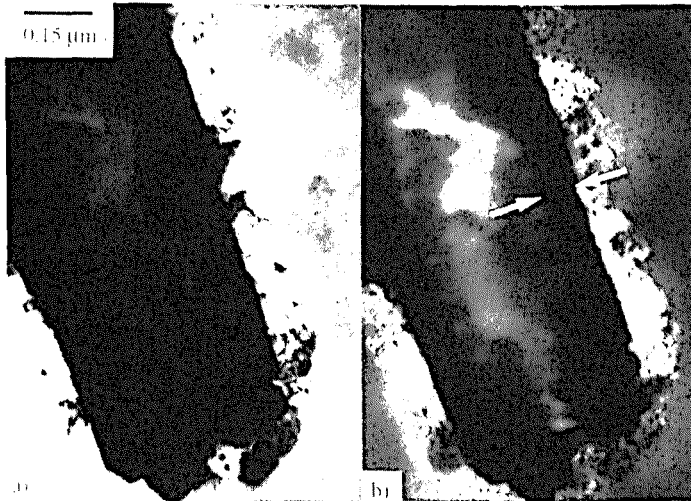


Figure 1. a) Bright-field-TEM of a TiB_2 particle in the as-quenched state of ribbon I with the $\langle 110 \rangle$ direction parallel to the electron beam. b) Dark-field-TEM with the objective aperture on the $\{111\}$ Al spot, reveals not only oriented Al-crystals but also an intermediate layer (arrows) surrounding the boride.

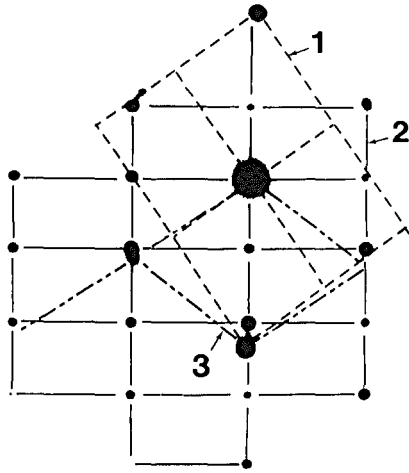


Figure 2. Selected area diffraction pattern of the boride in Figure 1 showing, with a slight tilt of the $\langle 110 \rangle$ boride zone axis, parts of (1) the $\langle 110 \rangle$ TiB₂, (2) the $\langle 110 \rangle$ Al₃Ti, and (3) the $\langle 110 \rangle$ Al patterns.

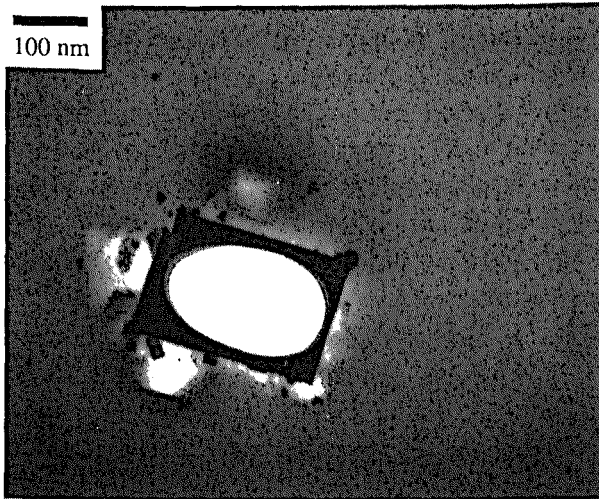


Figure 3. Boride particle with the $\langle 110 \rangle$ direction parallel to the electron beam in an as-quenched sample of ribbon II. No Al-crystals can be detected on the $\{001\}$ faces of the boride despite a less efficient quench than ribbon 2, suggesting that the boride is a much less effective nucleating agent.

In contrast to ribbon I, no copious formation of α -Al on boride particles can be found in the as-quenched state of ribbon II ($x \sim 0$; $y = 0.16$). This suggests either a more efficient quench and

therefore no nucleation and growth of α -Al, or that the negligible amount of excess Ti in the alloy is not sufficient to permit the formation of an Al_3Ti layer on boride particles, so that nucleation of α -Al can not take place on that layer. In the present work care has been taken to use as far as possible the same processing conditions for ribbon I and II; the relative quench-rates are assessed in the next section.

Isothermal anneals

The previous study [12] of the alloy without grain-refining additions showed, after partial devitrification, a microstructure with a bimodal size distribution of crystalline regions. The larger crystalline regions grew on active quenched-in nuclei, while the smaller regions appeared only after an incubation time and transformed the majority of the sample volume. This incubation time was found to be quench-rate dependent and to obey an Arrhenius relation with temperature. For identical annealing temperatures the ribbon with a slower quench exhibits a shorter incubation time. From the measured onset of the thermal signal exhibiting an incubation period in DSC it appears that ribbon I has a longer incubation time at 260°C ($t_{\text{inc I}} \sim 53$ min) than ribbon II ($t_{\text{inc II}} \sim 18$ min). Thus, despite the presence of copious formation of α -Al on $\{001\}$ boride faces in as-quenched samples of ribbon I, it appears that ribbon I is faster quenched than ribbon II. This strongly suggests that the presence of excess Ti is a necessity for a nucleation mechanism of α -Al on boride particles, as also empirically shown in grain refinement studies in Cibula's work [3]. In the present study the interest lies with nucleation and growth on boride particles rather than the remaining devitrification of the matrix, therefore a low annealing temperature is chosen at which the long incubation time for matrix devitrification permits the prolonged observation of the growth on heterogeneities. The evolution of microstructure at the borides has been studied in samples of ribbon I annealed for 20, 40, 50, 60 70 and 80 min at 260°C and ribbon II annealed for 5, 10, 15, and 20 min at 260°C . The thickness of the aluminide layer on the boride particles, and the effective thickness of the aluminium crystals forming on the boride, are measured perpendicular to the $\{001\}$ face of the boride particles. In ribbon II, even on annealing beyond the incubation period for matrix devitrification, there is no Al_3Ti layer and there is no clear evidence for heterogeneous nucleation on the borides; the small number of α -Al crystals found at the $\{001\}$ boride faces could be consistent with coincidental nucleation in the nearby matrix. In ribbon I, on the other hand, the α -Al crystals present in as-quenched samples appear to grow on annealing, linearly with time (see Figure 4). However, no clear conclusion can be drawn whether the Al grows diffusion-limited or not, since the early stages of growth happened during the quench. The aluminide layer on the boride particles appears not to thicken on annealing; this suggests that it is the product of reaction at higher temperatures in the melt.

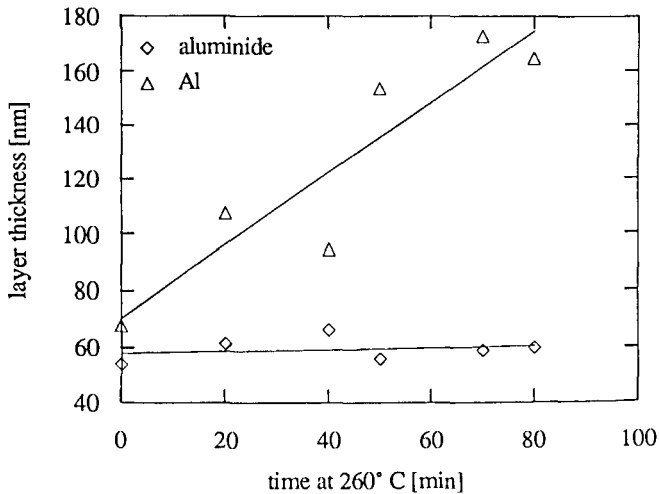


Figure 4. The aluminide layer and growth of α -Al on it are observed on borides only in ribbon I (with excess Ti). The development of layer thickness and α -Al growth are shown for annealing at 260° C.

Conclusion

Despite grain-refining additions to the melt, amorphous aluminium alloys can be produced by rapid quenching. However, even in melt-spinning, there can be some formation of α -Al particles on boride particles during the quench. The possibility has been demonstrated of studying induced heterogeneous nucleation in amorphous aluminium alloys. The nucleation of α -Al in this case is relevant for grain-refining in conventional processing of aluminium alloys. Preliminary studies have been made of the action of grain-refining particles and further studies are in progress. Of the particles known to be present in grain-refining rod, the borides are found in the amorphous alloys, but there is no trace of separate Al_3Ti particles, suggesting that they dissolve in the melt at the high temperatures before melt-spinning. With conventional Al-5wt.%Ti-1wt.%B refiner there is excess Ti (beyond the TiB_2 stoichiometry) and in this case an aluminide layer is found on the boride particles, formed presumably by high-temperature reaction in the melt. Crystallographic studies indicate that this is an Al_3Ti layer between the close-packed planes of the aluminium and the boride. On annealing, copious growth of α -Al occurs on the aluminide layer, but, even with the very high thermodynamic driving force for devitrification, crystallographic effects dominate; nucleation is only on the {001} faces of the boride particles. There are well defined orientation relationships between the phases, the close-packed planes and directions in each phase being

parallel. In contrast, with addition of Al-4.5wt.%Ti-1.8wt.%B which has nearly zero excess Ti, no aluminide and no copious heterogeneous nucleation of α -Al are found. These results support the hypothesis that boride particles promote nucleation in Al-melts by preserving an adsorbed layer of Al₃Ti. Hypotheses based on protective shells of borides or cavities in borides are not supported. The adsorbed layer appears to be formed in the melt only in the presence of excess Ti and it appears to be necessary for the nucleation of α -Al. These results are consistent with grain-refinement studies by Cibula [3] on dilute Al-melts. Many questions on grain refinement remain open, however, particularly on the mechanism of formation or preservation of the Al₃Ti layer and possible influences of solute in the aluminide layer on the nucleation mechanism for α -Al.

Acknowledgements

This work is supported by Alcan International Ltd (Banbury Laboratory) and by London & Scandinavian Metallurgical Co. Ltd.

References

- [1] L. Arnberg, L. Bäckerud and H. Klang, Grain refinement in Castings and Welds, ed. G.J. Abbaschian and S.A. David, AIME, Warrendale, 1983, 165.
- [2] T.W. Clyne and M.H. Robert, Metals Techn. 7, (1980), 177.
- [3] A. Cibula, J. Inst. Metals, 76, (1949), 323.
- [4] M. Vader and J. Noordegraaf, Light Metals 1990, ed.: C.M. Bickert The Minerals, Metals and Materials Society, 1990, 851.
- [5] L. Bäckerud, P. Gustafson and M. Johnson, Aluminium 67, (1991), 910.
- [6] D. Turnbull, J. Chem. Phys. 18, (1950), 198.
- [7] G. P. Jones, " New Ideas on the Mechanism of Heterogeneous Nucleation in Liquid Aluminium" (NPL Report, DMA (A) 19, National Physical Laboratory, Teddington, U.K., 1983).
- [8] P. Schumacher, Ph.D. thesis, University of Cambridge, UK (1994).
- [9] P. Schumacher and A.L. Greer, Mater. Sci. Eng. 178A, (1994), 309.
- [10] P. Schumacher and A.L. Greer, Mater. Sci. Eng. 181A, (1994), 1335.
- [11] A. Inoue, N. Matsumoto and T. Masumoto, Mater. Trans. JIM 6, (1990), 493.
- [12] P. Schumacher and A.L. Greer, Key Eng. Mater. 81-83, (1993), 631.
- [13] M. Johnson and L. Bäckerud, Z. Metallkd. 83, (1992), 11.
- [14] W.T. Kim, B. Cantor, W.D. Griffith and M.R. Jolly, Int. J. Rapid Solid. 7, (1992), 245.